Power Propagation in Homogeneous Isotropic Frequency-Dispersive Left-Handed Media

J. Pacheco, Jr., T. M. Grzegorczyk, B.-I. Wu, Y. Zhang, and J. A. Kong

Research Laboratory of Electronics, Massachusetts Institute of Technology, Cambridge, Massachusetts 02139-4307

(Received 23 May 2002; published 2 December 2002)

We study transmission at a boundary between a right-handed medium (RHM: $\epsilon > 0$, $\mu > 0$) and a frequency dispersive left-handed medium [LHM: $\epsilon(\omega) < 0$, $\mu(\omega) < 0$ for some ω], both homogeneous and isotropic. In order to account for the dispersion, two types of signal spectra are considered. The first consists of two discrete frequencies, while the second is Gaussian. Explicit expressions for the time-domain fields are obtained, from which the time-averaged Poynting vectors and hence power flow vectors are calculated. In both cases, we find that waves refract at negative angles at a RHM-LHM interface.

DOI: 10.1103/PhysRevLett.89.257401 PACS numbers: 78.20.Ci, 41.20.Jb, 41.85.Ew

The study of left-handed media (LHM), first introduced by Veselago in 1968 [1], has recently received much attention in the literature, both from a theoretical and an experimental point of view. Theoretically, such materials have been predicted to have a number of unique properties, including a negative index of refraction [2]. Although naturally occurring materials with simultaneously negative permittivity and permeability are not known, one left-handed material has been artificially realized as a periodic lattice of metallic rods and split-ring resonators. Theoretically, the rods have been shown to have an effective negative permittivity [3], while the split-ring resonators have been shown to have an effective negative permeability [4]. Experimentally, this metamaterial has been built and measured to have a negative index of refraction [5], consistent with theory [6]. Other negative index materials studied recently include photonic crystal structures [7] and transmission line networks [8].

More recently though, all previous theoretical predictions and experimental observations have been questioned by Valanju *et al.* [9], wherein the authors claim that the presence of dispersion prevents power transmitted at a RHM-LHM interface from refracting at a negative angle. Valanju *et al.* draw their conclusions based solely on the electric field inferring the direction of the power flow from the normal of the phase front. However, the direction of power flow for both nondispersive and dispersive media is determined by the Poynting vector, which is not necessarily parallel to the normal of the phase front [10]. It is the purpose of this Letter to address this issue by explicitly calculating the time and space dependent electric and magnetic fields due to a multifrequency incident wave transmitted into a frequency dispersive LHM. Indeed, from the resulting field expressions, the time-averaged Poynting vector is calculated and shown to refract at a negative angle, yet remaining causal.

In order to study the effect of dispersion on the direction of power propagation, we consider the transmission of an incident field, composed of many frequencies, from an isotropic nondispersive region into an isotropic dispersive region as shown in Fig. 1. The total TE polarized incident electric field is constructed as a weighted sum of plane waves and is given by

$$E_{0y}(\overline{r}, t) = \int_{-\infty}^{\infty} d\omega A(\omega) e^{i\phi_0(\overline{r},\omega) - i\omega t}, \tag{1}$$

where $A(\omega) = \alpha(\omega) + \alpha^*(-\omega)$ is the signal spectrum, $k_x(\omega) = k_0 \sin\theta_i$, $k_{0z}(\omega) = k_0 \cos\theta_i$, $k_0 = \omega\sqrt{\mu_0\epsilon_0}$, and $\phi_\ell(\overline{r}, \omega) = k_x(\omega)x + k_{\ell z}(\omega)z$, with ℓ referring to region 0 or 1. With this formulation, the transmitted electric field in region 1 is given by

$$E_{1y}(\overline{r}, t) = \int_{-\infty}^{\infty} d\omega A(\omega) T(\omega, \theta_i) e^{i\phi_1(\overline{r},\omega) - i\omega t}, \tag{2}$$

where $T(\omega, \theta_i)$ is the frequency and angle dependent transmission coefficient given by

$$T(\omega, \theta_i) = \frac{2\mu_1 k_{0z}}{\mu_1 k_{0z} + \mu_0 k_{1z}}, \tag{3}$$

and

$$k_{1z}(\omega) = \sigma\sqrt{\omega^2 \mu_1(\omega)\epsilon_1(\omega) - k_x^2(\omega)}, \tag{4}$$

where $\sigma = +1$ for RHM and $\sigma = -1$ for LHM. This choice of sign ensures power propagates away from the

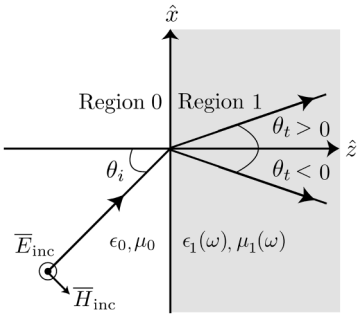

FIG. 1. Half-space problem geometry: A TE polarized incident wave is transmitted from a nondispersive region (0) into a dispersive region (1). Arrows shown here indicate power flow direction.

surface in the $+\hat{z}$ direction rather than from infinity [11]. From the electric field, we can calculate the magnetic field given by

$$H_{1z}(\overline{r}, t) = \int_{-\infty}^{\infty} d\omega \frac{k_x(\omega)}{\omega \mu_1(\omega)} A(\omega) T(\omega, \theta_i) e^{i\phi_1(\overline{r},\omega) - i\omega t}, \tag{5}$$

where for brevity we list only H_{1z}, noting that H_{1x} can be calculated in a similar manner.

In order to model a physically realizable narrow band signal, we first consider an incident field composed of two slightly separated frequencies with the following spectrum:

$$\alpha(\omega) = \frac{E_0}{2}[\delta(\omega - \omega_1) + \delta(\omega - \omega_2)], \tag{6}$$

where E_0 is the real-valued amplitude, $\omega_2 - \omega_1 = \delta\omega$, and $|\delta\omega/\omega_1| \ll 1$. From (2), we can find the expression for the time and space dependent transmitted electric field,

$$E_{1y}(\overline{r}, t) = E_0[\cos\psi_1 + \cos\psi_2], \tag{7}$$

where $\psi_j = \phi_1(\overline{r}, \omega_j) - \omega_j t$, with $j = 1, 2$. Note that, here we consider the lossless case and let $T(\omega, \theta_i) = 1$ for the simplicity of derivation. Later in this Letter we will consider a more rigorous derivation that includes the transmission coefficient. To proceed with the Poynting vector calculation, we first determine the magnetic field, which is given by

$$H_{1z}(\overline{r}, t) = E_0\left[\frac{k_x(\omega_1)\cos\psi_1}{\omega_1\mu_1(\omega_1)} + \frac{k_x(\omega_2)\cos\psi_2}{\omega_2\mu_1(\omega_2)}\right], \tag{8}$$

where again for brevity we list only H_{1z}. To find the power flow direction, we calculate the time and space dependent Poynting vector, given by $\overline{S}_1(\overline{r}, t) = \overline{E}_1(\overline{r}, t) \times \overline{H}_1(\overline{r}, t)$, yielding

$$S_{1x}(\overline{r}, t) = E_0^2 \frac{k_x(\omega_1)}{\omega_1\mu_1(\omega_1)}\cos^2\psi_1 + E_0^2 \frac{k_x(\omega_2)}{\omega_2\mu_1(\omega_2)}\cos^2\psi_2 + E_0^2\left[\frac{k_x(\omega_1)}{\omega_1\mu_1(\omega_1)} + \frac{k_x(\omega_2)}{\omega_2\mu_1(\omega_2)}\right]\cos\psi_1\cos\psi_2, \tag{9}$$

where we note that a similar calculation for S_{1z} can also be done. In order to determine the power propagation direction, we calculate the time average value of the time dependent Poynting vector by integrating (9) and a similar expression for S_{1z} over a period T, which is chosen to be the period of the combined signal, i.e., it is the common period of the frequencies $\omega_1 + \omega_2$ and $\omega_1 - \omega_2$. Integrating, we find that the cross terms average to zero if $\omega_1 \neq \omega_2$ yielding

$$\langle \overline{S}_1(\overline{r}, t)\rangle = \frac{E_0^2}{2}\left[\frac{\overline{k}_1(\omega_1)}{\omega_1\mu_1(\omega_1)} + \frac{\overline{k}_1(\omega_2)}{\omega_2\mu_1(\omega_2)}\right], \tag{10}$$

where $\overline{k}_1(\omega) = \hat{x}k_x(\omega) + \hat{z}k_{1z}(\omega)$. From this expression, we see that the power flow will be in the average direction of the two single frequencies. Thus, depending on the values of $\mu_1(\omega_1)$, $\mu_1(\omega_2)$, $\epsilon_1(\omega_1)$, and $\epsilon_1(\omega_2)$ the wave will refract at either a positive or a negative angle. In the case that both the permittivities and permeabilities at each frequency are negative, the wave will refract at a negative angle.

We will now consider two specific simple examples. The first example is the transmission of a wave with two frequency components at $f_1 = 10.5$ GHz and $f_2 = 11.5$ GHz ($\omega = 2\pi f$) where we take the permittivity for region 1 to be different for each frequency, yet both positive, while the permeability remains fixed and positive such that in this example, both regions are RHM. The second example is the case of transmission from a RHM to a LHM where we again take the permittivity for region 1 to be different for each frequency, yet both negative, while the permeability remains fixed and negative. Figure 2 for the first example and Fig. 3 for the second example show, at a specific time, the resulting $\hat{x}$ component of the Poynting vector, overlayed with white colored arrows that indicate the overall direction of the vector. Clearly, in the case of the RHM-RHM interface, the $\hat{x}$ component of the Poynting vector is positive, while in the RHM-LHM case the $\hat{x}$ component is negative. Hence, as can be seen from the arrows, $\theta_t > 0$ for the RHM-RHM interface and $\theta_t < 0$ for the RHM-LHM interface. Note that calculation of the Poynting vector for subsequent times shows that the time-averaged S_x component is positive for the RHM-RHM case and negative for the RHM-LHM case, as predicted by (10).

Note, however, that in both cases an interference pattern is formed whose normal vectors are not in the direction of the respective power flows. This interference is a result of the fact that the waves for each frequency are refracted at different angles. From the above calculations we see that, contrary to the conclusions in [9], the normal vectors of these interference fronts do not indicate the power flow direction.

Next, in order to more rigorously model a physically realizable narrow band signal, we consider an incident field with a normalized Gaussian signal spectrum,

$$\alpha(\omega) = \frac{E_0}{\sqrt{4\pi(\delta\omega)^2}}\exp\left[-\frac{(\omega - \omega_0)^2}{(\delta\omega)^2}\right], \tag{11}$$

where as before E_0 is the real-valued amplitude, and $|\delta\omega/\omega_0| \ll 1$. The time-domain expressions for the fields given in (2) and (5) involve the evaluation of integrals that can be dealt with using a standard expansion method. Note that, by conjugate symmetry, we need only integrate the portion of the spectrum centered at ω_0. A generic form of the integral is given by

$$I = \int_{-\infty}^{\infty} d\omega f(\omega) e^{i\gamma(\omega)} = \int_{-\infty}^{\infty} d\omega e^{g(\omega)}, \tag{12}$$

where $g(\omega) = i\gamma(\omega) + \ln[f(\omega)]$ and the principle branch of the logarithm function is taken. To evaluate this

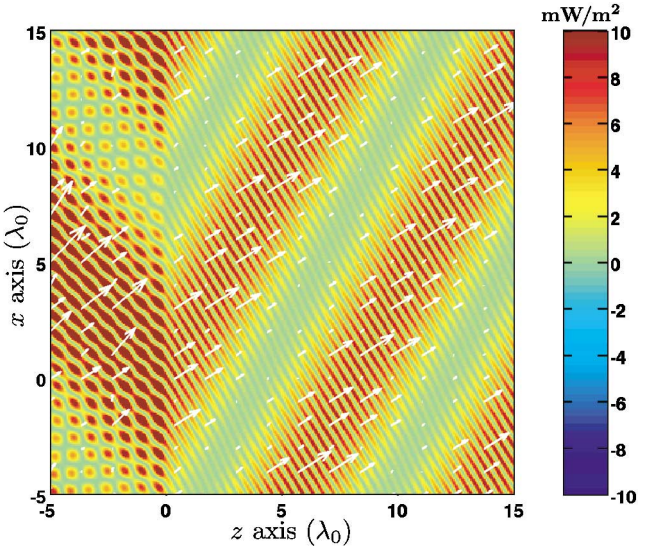

FIG. 2 (color). RHM-RHM interface: S_x component overlayed with arrows indicating the direction and magnitude of the Poynting vector at a specific time for a wave incident at $\theta_i = 45°$ composed of two discrete frequencies, $f_1 = 10.5$ GHz and $f_2 = 11.5$ GHz with $\epsilon_{1r}(\omega_1) = 2$, $\epsilon_{1r}(\omega_2) = 1.5$, and $\mu_{1r}(\omega_1) = \mu_{1r}(\omega_2) = 1$. λ_0 corresponds to the wavelength of the mean frequency.

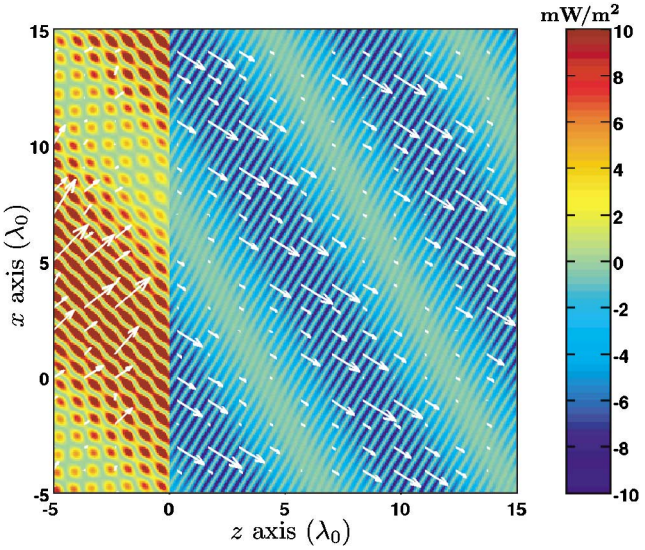

FIG. 3 (color). RHM-LHM interface: Similar to Fig. 2 except $\epsilon_{1r}(\omega_1) = -2$, $\epsilon_{1r}(\omega_2) = -1.5$, and $\mu_{1r}(\omega_1) = \mu_{1r}(\omega_2) = -1$.

integral, the argument to the exponential, $g(\omega)$, is expanded in a Taylor series about ω_0 to second order to yield

$$I = \sqrt{\frac{2\pi}{g''(\omega_0)}} \exp\left[g(\omega_0) - \frac{[g'(\omega_0)]^2}{2g''(\omega_0)} \right]. \tag{13}$$

Note that, in the case of nondispersive media, the second order Taylor series expansion is exact. For dispersive media, this approximation holds as long as the signal spectrum $\alpha(\omega)$ spans only a linear portion of the dispersion curve, which is true outside the region of resonance, under the condition $|\delta\omega/\omega_0| \ll 1$. Note that there is no loss of generality by limiting the spectrum in this manner since group velocity and power flow direction are determined by considering the local slope of the dispersion curve [12].

In order to apply this method to determine the fields in region 1, we specify definitions of $g(\omega)$, depending on the field component examined, e.g.,

$$g_{E_{1y}}(\omega) = -\frac{(\omega - \omega_0)^2}{(\delta\omega)^2} + \ln[T(\omega)] + i[k_x(\omega)x + k_{1z}(\omega)z - \omega t], \tag{14a}$$

$$g_{H_{1z}}(\omega) = -\frac{(\omega - \omega_0)^2}{(\delta\omega)^2} + \ln[T(\omega)] + \ln\left[\frac{k_x(\omega)}{\omega\mu_1(\omega)}\right] + i[k_x(\omega)x + k_{1z}(\omega)z - \omega t]. \tag{14b}$$

As an example, we consider the following dispersion relations given by Shelby *et al.* [5]:

$$\frac{\mu_1(\omega)}{\mu_0} = 1 - \frac{\omega_{mp}^2 - \omega_{mo}^2}{\omega^2 - \omega_{mo}^2 + i\gamma\omega}, \tag{15a}$$

$$\frac{\epsilon_1(\omega)}{\epsilon_0} = 1 - \frac{\omega_{ep}^2 - \omega_{eo}^2}{\omega^2 - \omega_{eo}^2 + i\gamma\omega}, \tag{15b}$$

where ω_{mo} is the magnetic resonance frequency, ω_{mp} is the magnetic plasma frequency, ω_{eo} is the electric resonance frequency, ω_{ep} is the electric plasma frequency, and γ is the loss factor. Explicit analytical expressions for the electric and magnetic fields are derived from the use of (13) and (14), but are not listed for the sake of brevity.

To proceed with a numerical evaluation of the electric and magnetic fields, the parameters reported in [5] are used, except with $\gamma = 0$ in order to suppress losses for the purpose of illustration. The incident wave is chosen to have a Gaussian spectrum centered at $f_0 = 10.5$ GHz with $\delta f = 10$ Hz, and is incident at $\theta_i = 45°$. From the resulting time-domain electric and magnetic fields, the Poynting vector is calculated. Figure 4 shows the S_{1x} and S_{1z} components as a function of time for one typical spatial point in the LHM region. The dot-dashed curve shows that the $\hat{x}$ component of the power is indeed always negative indicating a negative angle of refraction. Specifically, this angle can be calculated by applying

$$\theta_t = \tan^{-1}\left[\frac{\langle S_{1x}(t)\rangle}{\langle S_{1z}(t)\rangle}\right]. \tag{16}$$

In the example shown in Fig. 4, θ_t is found to be approximately $-11.12°$. For comparison, note that at the center frequency, $\epsilon_{1r}(\omega_0) \approx -12.88$ and $\mu_{1r}(\omega_0) \approx -1.04$, which corresponds to an index of refraction $n(\omega_0) \approx -3.67$ and a refraction angle of $\theta_t \approx -11.12°$. Hence, comparing these two values we conclude that dispersion

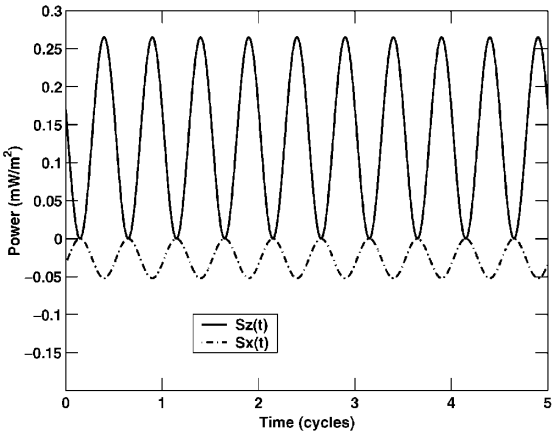

FIG. 4. S_{1x} and S_{1z} at one typical spatial point in the LHM region as a function of time. Center frequency is $f_0 = 10.5$ GHz with $\delta f = 10$ Hz. Parameters used were those reported in [5], $f_{mp} = 10.95$ GHz, $f_{mo} = 10.05$ GHz, $f_{ep} = 12.8$ GHz, $f_{eo} = 10.3$ GHz, except $\gamma = 0$. Refraction angle is found to be $\theta_t \approx -11.12°$.

does not preclude refraction at a negative angle in accordance with Snell's law. It should be noted that the power plotted in Fig. 4 is not strictly periodic since a continuum of frequencies is used; however, this fact does not affect the conclusion that the power is refracted at a negative angle.

Additionally, it can be seen that negative refraction does not violate causality. The argument presented in [9] fails to consider two important points. First, at a RHM-RHM interface, points on a single phase front in the incident region can all be mapped to the same phase front in the transmitted region; however, this is not the case for a RHM-LHM interface. Instead, the points along the incident phase fronts are each mapped to different backward propagating phase fronts in the LHM. Second, in the case of a single frequency signal, for which constant phase front arguments apply, it is always possible to form new backward propagating phase fronts due to the negative phase property of LHM in conjunction with the fact that the wave exists for all time and space. Considering these two points, we see that waves can refract at negative angles while maintaining a finite velocity.

On the other hand, the interference fronts of a multifrequency signal are indeed distorted at a RHM-LHM interface since its different frequency components are refracted at different angles. In the case of two discrete frequencies, examples of two distorted interference patterns are shown in Figs. 2 and 3. Valanju *et al.* argue that these distorted interference patterns move and carry power perpendicularly to the interference front, which happens to be at a positive angle in the case considered in Fig. 3. In actuality, each point on the interference front moves in the direction of power flow (downward and to the right in Fig. 3). The apparent upward movement is due to the combined effects of semi-infinite extent, the periodicity of the interference pattern, and its slanted angle. Indeed, a spatially finite extent signal such as a Gaussian beam, which can be represented by a collection of plane waves [13], will also propagate downwards in this case since each plane wave component will refract negatively. The combined effects listed above along with the exact analytical calculation of the power flow presented in this Letter demonstrate that conclusions based solely on the apparent motion of the interference fronts are misguided.

In conclusion, we have calculated the power flow of a wave transmitted from a nondispersive right-handed medium into a dispersive medium, both RHM and LHM. In particular, we have shown that negative refraction is possible for multifrequency signals by explicit calculation of the Poynting vector in LHM. Using two discrete frequencies, we have shown that the direction of the time-averaged Poynting vector is in the average direction of the time-averaged Poynting vectors for each frequency treated separately, implying that negative refraction is possible. Using a Gaussian signal spectrum, we have confirmed this conclusion after also determining the power refraction angle to be negative, without violating causality. The angle of refraction was found to be in agreement with that predicted by Snell's law, with the LHM having a negative index of refraction.

This work was supported in part by the MIT Lincoln Laboratory under Contract No. BX-8133 and the Office of Naval Research under Contracts No. N00014-10-1-0713 and No. N00014-99-1-0175.

[1] V. G. Veselago, Sov. Phys. Usp. **10**, 509 (1968).
[2] J. B. Pendry, Phys. Rev. Lett. **85**, 3966 (2000).
[3] J. B. Pendry, A. J. Holden, W. J. Stewart, and I. Youngs, Phys. Rev. Lett. **76**, 4773 (1996).
[4] J. B. Pendry, A. J. Holden, D. J. Robbins, and W. J. Stewart, IEEE Trans. Microwave Theory Tech. **47**, 2075 (1999).
[5] R. A. Shelby, D. R. Smith, and S. Schultz, Science **292**, 77 (2001).
[6] D. R. Smith and N. Kroll, Phys. Rev. Lett. **85**, 2933 (2000).
[7] M. Notomi, Phys. Rev. B **62**, 10 696 (2000).
[8] A. K. Iyer and G. V. Eleftheriades, in *Proceedings of the IEEE MTT-S International Microwave Symposium Digest* (IEEE, Piscataway, NJ, 2002), Vol. 2, pp. 1067–1070.
[9] P. M. Valanju, R. M. Walser, and A. P. Valanju, Phys. Rev. Lett. **88**, 187401 (2002).
[10] L. D. Landau, E. M. Lifshitz, and L. P. Pitaevskii, *Electrodynamics of Continuous Media* (Pergamon Press, New York, 1984).
[11] R. Ziolkowski and E. Heyman, Phys. Rev. E **64**, 056625 (2001).
[12] L. Brillouin, *Wave Propagation and Group Velocity* (Academic Press, New York, 1960).
[13] J. A. Kong, B.-I. Wu, and Y. Zhang, Appl. Phys. Lett. **80**, 2084 (2002).